SMALL RNA DECAY

Tudor-SN–mediated endonucleolytic decay of human cell microRNAs promotes G_1/S phase transition

Reyad A. Elbarbary,[1,2]* Keita Miyoshi,[1,2]* Jason R. Myers,[3] Peicheng Du,[4] John M. Ashton,[3] Bin Tian,[5] Lynne E. Maquat[1,2,6]†

MicroRNAs (miRNAs) are small noncoding RNAs that regulate gene expression. The pathways that mediate mature miRNA decay are less well understood than those that mediate miRNA biogenesis. We found that functional miRNAs are degraded in human cells by the endonuclease Tudor-SN (TSN). In vitro, recombinant TSN initiated the decay of both protein-free and Argonaute 2–loaded miRNAs via endonucleolytic cleavage at CA and UA dinucleotides, preferentially at scissile bonds located more than five nucleotides away from miRNA ends. Cellular targets of TSN-mediated decay defined using microRNA sequencing followed this rule. Inhibiting TSN-mediated miRNA decay by CRISPR-Cas9 knockout of TSN inhibited cell cycle progression by up-regulating a cohort of miRNAs that down-regulates mRNAs that encode proteins critical for the G_1-to-S phase transition. Our study indicates that targeting TSN nuclease activity could inhibit pathological cell proliferation.

Human TSN is an evolutionarily conserved nuclease that contains five staphylococcal/micrococcal-like nuclease (SN) domains and a Tudor domain, which generally mediates protein-protein interactions. Bacterial homologs of TSN degrade RNA in vitro via endonucleolytic cleavage, which generates a 3′-phosphate, followed by 3′-to-5′ exonucleolytic cleavages, yielding mono- and dinucleotides (*1*). In mammals, TSN is a multifunctional protein implicated in the degradation of double-stranded RNAs harboring multiple A-to-I edited sites (*2*) and inosine-containing primary miRNAs (pri-miRNAs) (*3*). Although TSN was the first RNA-induced silencing complex (RISC) subunit characterized as having endonuclease activity (*4*), subsequent reports demonstrating that Argonaute 2 (AGO2) is the RISC catalytic component (*5*) spurred us to identify TSN function in RISC.

We first confirmed that cellular TSN coimmunoprecipitates with the RISC components AGO2 and trinucleotide repeat–containing 6A (also known as GW182) in a largely RNase I (ribonuclease I)–resistant fashion (fig. S1A and table S1). We corroborated this result by detecting cellular TSN in the reciprocal immunoprecipitation of FLAG-tagged AGO2 (fig. S1B).

To determine whether RISC-associated TSN functions in miRNA metabolism, we quantitated the levels of select miRNAs and their precursor miRNAs (pre-miRNAs) and pri-miRNAs in human embryonic kidney (HEK) 293T cells transfected with TSN small interfering RNA (siRNA) relative to control (Ctl) siRNA (fig. S2A). Reverse transcription quantitative polymerase chain reaction (RT-qPCR) and Northern blotting demonstrated that TSN knockdown up-regulates the abundance of mature miR-31-5p, miR-29b-3p, and miR-125a-5p without significantly changing the levels of their pre- or pri-miRNAs (Fig. 1A and fig. S2B). TSN knockdown did not alter the abundance of mature miR-3648 and miR-128-3p (fig. S2C), which suggests that these effects are not generalizable to all miRNAs. These same miRNA-specific results were observed with HeLa cells (fig. S2D).

TSN targets functional miRNAs, as evidenced by the finding that TSN knockdown and the consequential accumulation of miR-31-5p and miR-29b-3p (Fig. 1A) are accompanied by decreased expression of integrin α5 (ITGA5) and lysyl oxidase (LOX) (fig. S3A), which are encoded by their respective mRNA targets (*6*, *7*) (fig. S3, B to E). The decreased level of ITGA5 and LOX was restored by expressing a miR-31-5p inhibitor or a miR-29b-3p inhibitor, respectively (fig. S3A); this result confirmed that the observed TSN regulation is miRNA-mediated.

The increased abundance of miRNAs and their mRNA-targeting activities upon TSN knockdown is not due to enhanced loading of miRNAs into AGO2. This was made clear by programming FLAG-AGO2 in lysates of HEK293T cells, which stably express FLAG-AGO2 and had been transiently transfected with Ctl or TSN siRNA (fig. S3F), with 5′-[^{32}P]-miR-31-5p (fig. S3G). Immunoprecipitations of FLAG-AGO2 revealed that TSN knockdown did not increase the level of 5′-[^{32}P]-miR-31-5p in FLAG-AGO2 (fig. S1C).

Additional support for TSN promoting miRNA turnover derives from our finding that TSN knockdown increased the abundance of miR-31-5p, miR-29b-3p, and miR-125a-5p when miRNA biogenesis was inhibited by conditional Dicer knockdown (Fig. 1, B and C, and fig. S4, A to C), but showed no effect on the corresponding miR* (i.e., the less abundant strand of the Dicer-generated duplex) (fig. S4D). Furthermore, TSN knockdown increased the abundance of miR-31-5p that derived from an exogenously introduced miR-31-5p mimic (Fig. 1D), indicating that TSN-mediated miRNA turnover does not require Drosha- or Dicer-dependent processing steps that precede miR:miR* duplex formation. We term this TumiD (i.e., Tudor SN–mediated miRNA decay). TumiD adds a new dimension to reports that miRNA stability can be regulated by exonucleases and complementarity to target mRNAs (*8*).

TumiD requires TSN nuclease activity, as evidenced by the ability of wild-type TSN^R, but not catalytically inactive TSN^R(ΔSN1) or TSN^R(ΔSN4) (fig. S4, E to I), to rescue the TumiD activity of cellular TSN (Fig. 1E). Moreover, incubating HEK293T cells with 2′-deoxythymidine-3′,5′-bisphosphate (pdTp), a general inhibitor of staphylococcal nucleases (*9*) (fig. S4J), at a concentration (200 μM) that inhibits TSN nuclease activity in human cells (*10*) increased the abundance of TumiD targets (fig. S4K).

Two independent microRNA sequencing (miR-seq) experiments—runs 1 and 2, each in biological triplicate—expanded the number of cellular TumiD targets. Upon TSN knockdown, the levels of 49 and 88 miRNAs were significantly up-regulated (adjusted P value < 0.05) in runs 1 and 2, respectively, of which 35 were common to both experiments (Fig. 2A, figs. S5 to S10, and tables S2 to S4).

Nine of 10 chosen miRNAs that were significantly up-regulated in both runs (Fig. 2A and table S4) proved to be bona fide TumiD targets (Fig. 2B and fig. S11A). Evaluation of the tenth, miR-221-3p, was obscured by up-regulation of its pri-mRNA upon TSN knockdown (fig. S11B). Using miR-seq and RT-qPCR, we demonstrated that TSN knockdown did not alter the abundance of the miR* for miR-125a-5p, miR-99b-5p, or miR-98-5p (fig. S11C and table S3), thereby providing additional evidence that TumiD degrades mature miRNAs. Note that the miR* of some TumiD targets is itself a TumiD target, as exemplified by miR-126-5p (Fig. 2, A and B, and tables S3 and S4).

TumiD also contributes to the differential regulation of the six miR-17-92 cluster–derived miRNAs (*11*) (fig. S11, D and E, and table S3) and of the miR-15a/16-1 and miR-23a/27a/24-2 cluster-derived miRNAs (fig. S12, A to C, and table S3). Notably, miRNA members of each cluster have distinct functions in development and disease.

TSN preferentially cleaves at CA and UA dinucleotides, as revealed when 5′-[^{32}P]-miR-31-5p, 5′-[^{32}P]-miR-29b-3p, or 5′-[^{32}P]-miR-126-3p was incubated with recombinant histidine-tagged

[1]Department of Biochemistry and Biophysics, School of Medicine and Dentistry, University of Rochester, Rochester, NY 14642, USA. [2]Center for RNA Biology, University of Rochester, Rochester, NY 14642, USA. [3]Genomics Research Center, University of Rochester, Rochester, NY 14642, USA. [4]Office of Advanced Research Computing, Rutgers University, Piscataway, NJ 08854, USA. [5]Department of Microbiology, Biochemistry, and Molecular Genetics, Rutgers New Jersey Medical School, Newark, NJ 07103, USA. [6]Department of Oncology, School of Medicine and Dentistry, University of Rochester, Rochester, NY 14642, USA.
*These authors contributed equally to this work. †Corresponding author. Email: lynne_maquat@urmc.rochester.edu

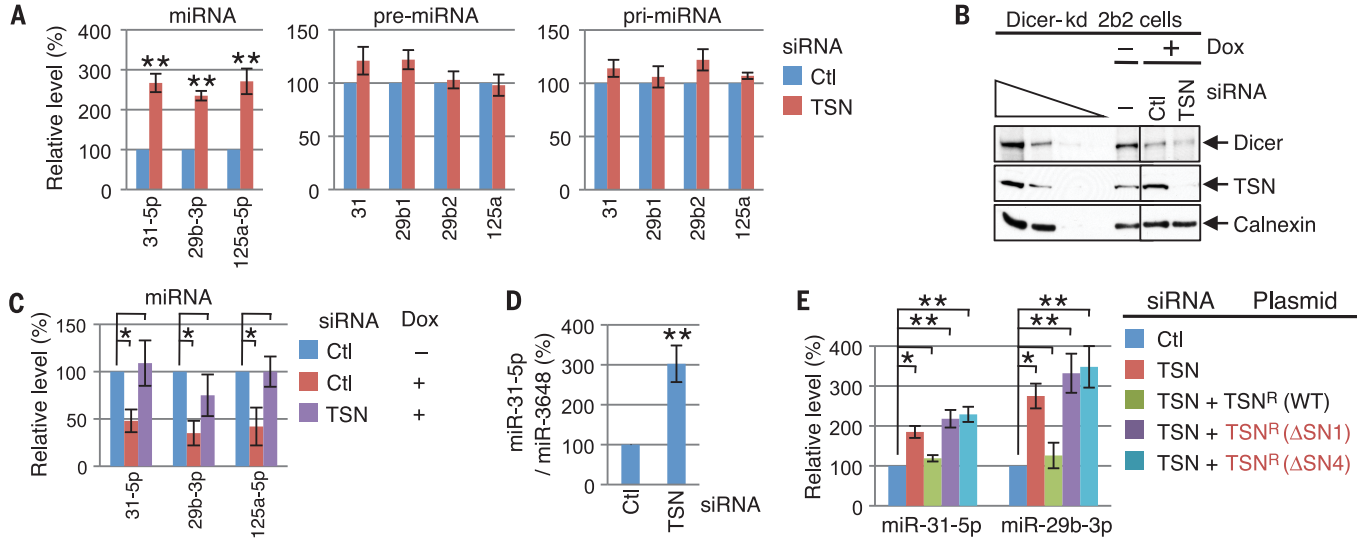

Fig. 1. TSN mediates cellular degradation of mature and biologically active miRNAs. (**A**) RT-qPCR revealing that mature miRNA levels increased in cells transfected with TSN siRNA relative to Ctl siRNA, while the corresponding pre- or pri-miRNA levels remained unchanged. (**B**) Western blot showing that exposing Dicer-kd 2b2 cells (*20*) to doxycycline (Dox) to induce Dicer short hairpin RNA (shRNA) production inhibits Dicer expression. Cells were transfected with Ctl or TSN siRNA and exposed to Dox for 4 days before harvesting. (**C**) RT-qPCR of RNA from (B) demonstrating that when doxycycline is used to inhibit miRNA biogenesis, miRNAs are stabilized by TSN siRNA relative to Ctl siRNA. (**D**) RT-qPCR showing that TSN siRNA up-regulates the level of exogenously introduced miR-31-5p relative to the level of co-introduced miR-3648. (**E**) RT-qPCR showing that wild-type TSN^R, but not the catalytically inactive variant TSN^R(ΔSN1) or TSN^R(ΔSN4), rescues the activity of cellular TSN. Here and elsewhere, all results derive from three or more independent experiments. For RT-qPCR results, miRNA and pre-miRNA levels are relative to U6 snRNA, pri-miRNA levels are relative to β-actin mRNA, and relative levels in the presence of Ctl siRNA are defined as 100. Histograms represent the average and SD. *P < 0.05, **P < 0.01.

TSN (HIS-TSN) and reaction products were analyzed in sequencing gels (Fig. 3A and fig. S13A). Endonucleolytic cleavage was followed by 3′-to-5′ exonucleolytic degradation (Fig. 3A and fig. S13A), as is typical for the mode of the bacterial homolog of TSN, micrococcal nuclease (*1*). miR-3648, which lacks CA and UA, was resistant to HIS-TSN–mediated degradation (fig. S13B), as was a hybrid miRNA generated by swapping a cleavable CA-containing region of miR-31-5p with a region from miR-3648 (fig. S13C, compare to Fig. 3A). HIS-TSN–mediated degradation depended on Ca^{2+} (fig. S13B) and was inhibited by converting the phosphodiester bond of a susceptible dinucleotide to a phosphorothioate bond (Fig. 3, B and C, and fig. S14), which has lower affinity for Ca^{2+} (*9*). Inserting a CA dinucleotide into HIS-TSN–resistant miR-3648 induced cleavage at the inserted CA (fig. S15), and cleavage was least optimal at CA dinucleotides situated within the five 5′-most or five 3′-most nucleotides of a miRNA (fig. S16, A and B). Consistent with this finding, when the 11 3′-most nucleotides of miR-29b-3p were swapped for the corresponding region of miR-150-3p (which contains a CA in the five 3′-most nucleotides), cleavage in the swapped region was abolished (fig. S16, C and D, compare to Fig. 3A).

Investigating cellular TumiD revealed that artificially inserting CA dinucleotides into TumiD-resistant miR-3648 at two positions favorable for TSN cleavage in vitro (fig. S17A) converted the miRNA to a TumiD target (fig. S17B). Of the 35 miRNAs that were significantly up-regulated upon TSN knockdown in both miR-seq runs (table S4), the two lacking CA or UA were up-regulated

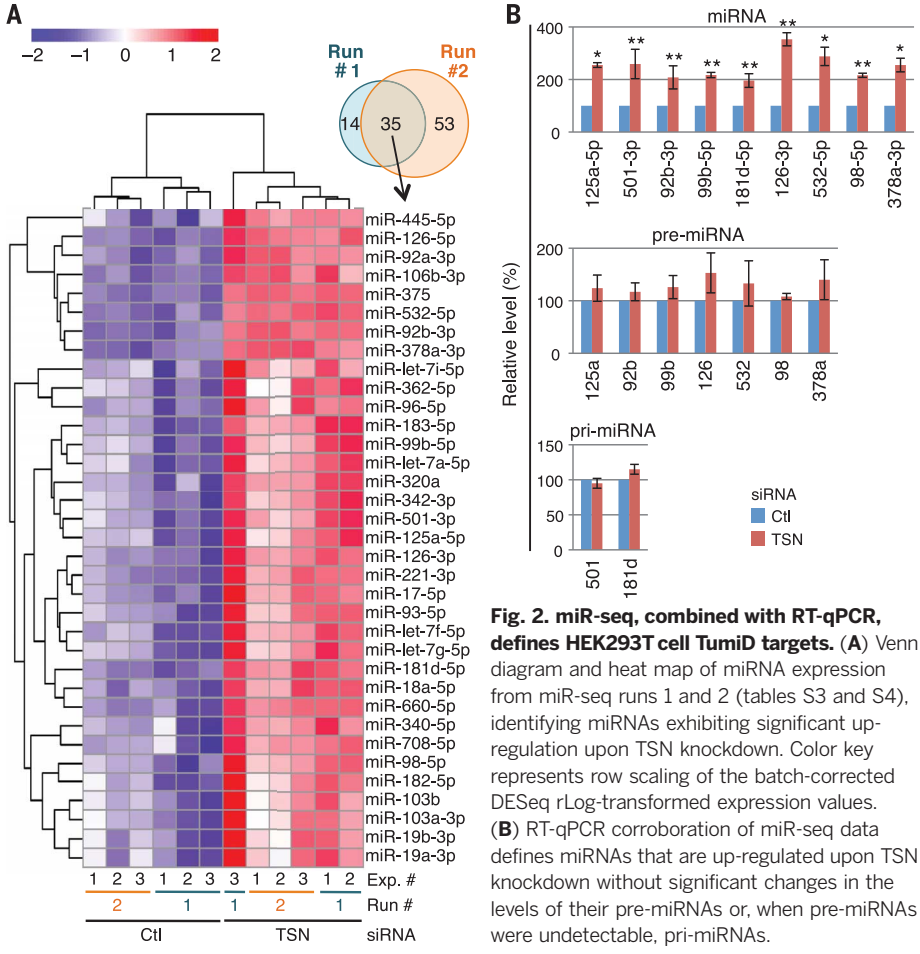

Fig. 2. miR-seq, combined with RT-qPCR, defines HEK293T cell TumiD targets. (**A**) Venn diagram and heat map of miRNA expression from miR-seq runs 1 and 2 (tables S3 and S4), identifying miRNAs exhibiting significant up-regulation upon TSN knockdown. Color key represents row scaling of the batch-corrected DESeq rLog-transformed expression values. (**B**) RT-qPCR corroboration of miR-seq data defines miRNAs that are up-regulated upon TSN knockdown without significant changes in the levels of their pre-miRNAs or, when pre-miRNAs were undetectable, pri-miRNAs.

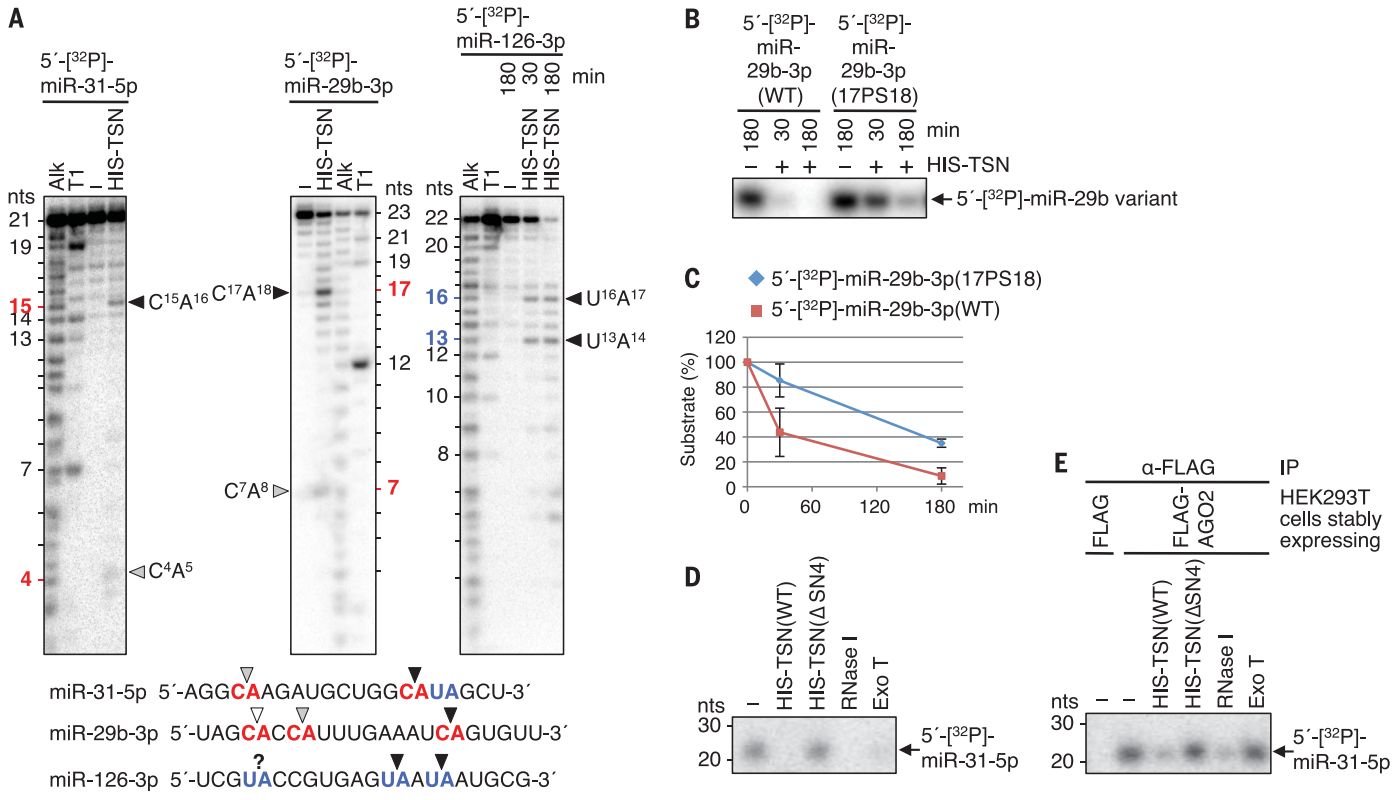

Fig. 3. TSN degrades naked and AGO2-loaded miRNAs at CA and UA dinucleotides in vitro. (**A**) Phosphorimages of sequencing gels reveal that recombinant TSN cleaves protein-free 5′-[^{32}P]-labeled miRNAs at CA and UA. Alk, alkaline hydrolysis to generate a ladder of nucleotides (nts); T1, RNase T1 digestion to generate a ladder of nucleotides cleaved after guanines; (–), no HIS-TSN. Black, gray, and white arrowheads respectively denote strong, medium, and weak cleavage sites. Unlabeled bands are decay intermediates resulting from TSN exonuclease activity since they were not detectable upon 3′-[^{32}P]Cp-labeled miRNA incubation with HIS-TSN (fig. S13A). (**B**) Replacing a susceptible CA phosphodiester bond in protein-free 5′-[^{32}P]-miR-29b-3p with a CA phosphorothioate bond inhibits HIS-TSN–mediated degradation. WT, wild type; 17PS18, phosphorothioate bond between nucleotides 17 and 18. (**C**) Plot of results shown in (B). The amount of each 5′-[^{32}P]-labeled miRNA in the absence of HIS-TSN is defined as 100. (**D**) Protein-free 5′-[^{32}P]-miR-31-5p (–) is degraded by HIS-TSN(WT), endonuclease RNase I, or 3′-to-5′ exonuclease Exo T but not catalytically inactive (fig. S4G) HIS-TSN(ΔSN4). (**E**) FLAG-AGO2–loaded 5′-[^{32}P]-miR-31-5p is protected from degradation by Exo T and is susceptible to degradation by HIS-TSN(WT) and RNase I but not by HIS-TSN(ΔSN4).

before miRNA generation (fig. S17C); the remaining 33 contained CA and/or UA at favorable positions for TSN cleavage. Notably, 31 mouse miRNAs that we identified as orthologs of putative or proven human TumiD targets that were up-regulated upon TSN knockdown in both runs are themselves predicted to be TumiD targets and have CA and/or UA dinucleotides at the same position(s) (table S5).

We are underestimating the number of cellular TumiD targets, because miRNAs with half-lives sufficiently long to preclude a detectable change during the period of TSN knockdown will escape definition. We limited our analyses to ≤4 days after transient transfection using TSN siRNA because longer transient knockdown or constitutive knockout (KO) of TSN inhibits cell cycle progression (see below). Moreover, unknown factors must affect the specificity of cellular TumiD, given that short-lived miR-503-5p (*12*) is not a TumiD target despite harboring an internal CA (fig. S17D).

AGO2-loaded miRNAs are protected from 3′-to-5′ exonucleolytic degradation by bacterial exonuclease T (Exo T). However, we found that they were susceptible to endonucleolytic degradation mediated by bacterial RNase I, which cleaves between any two nucleotides, or HIS-TSN (Fig. 3, D and E, and figs. S4G and S18).

To assess whether TSN facilitates the G_1/S-phase transition in human cells as it does in mouse embryonic fibroblasts (*13*), we established two independent stable TSN KO HEK293T cell lines using CRISPR, the D10A nickase variant of Cas9 (*14*), and, to control for off-target effects of CRISPR-Cas9, different pairs of single guide RNAs (fig. S19). Synchronizing wild-type and TSN KO cells at G_2/M using nocodazole, or at G_1/S using a double-thymidine block followed by flow cytometry analysis after release from synchronization, revealed a prolonged cell cycle in both TSN KO cell lines (TSN KO 1 or 2) due to slow progression through the G_1/S transition (Fig. 4A and fig. S20). Stably expressing FLAG-TSN in each TSN KO cell line rescued the pace of G_1/S progression (fig. S21, A and B). Consistent with results from transient TSN knockdowns (Fig. 1A and fig. S11E), the levels of the TumiD targets miR-31-5p, miR-17-5p, and miR-20a-5p were significantly up-regulated in G_1/S in both TSN KO cell lines relative to wild-type cells (Fig. 4B and fig. S22A).

Using miRNA mimics, we confirmed previous reports (*15*–*18*) that these three TumiD targets down-regulate the expression of genes critical for G_1/S transition: Cyclin-dependent kinase 2 (*CDK2*) mRNA was down-regulated by a miR-31-5p mimic, both cyclin D1 (*CCND1*) and E2F transcription factor 1 (*E2F1*) mRNAs were separately down-regulated by a miR-17-5p mimic and a miR-20a-5p mimic, and *E2F2* mRNA was down-regulated by a miR-20a-5p mimic (fig. S22B). Consistent with these results, increased G_1/S levels of the three miRNAs in TSN KO cells were accompanied by decreased levels of their target *CDK2*, *CCND1*, *E2F1*, and *E2F2* mRNAs (Fig. 4C and fig. S22C) and target-encoded proteins (fig. S22D). Furthermore, transfecting TSN KO cells with miRNA inhibitors rescued the levels of *CDK2*, *CCND1*, *E2F1*, and *E2F2* mRNAs (Fig. 4C and fig. S22C) and their corresponding proteins (fig. S22D), indicating that TSN regulates the expression of these cell cycle

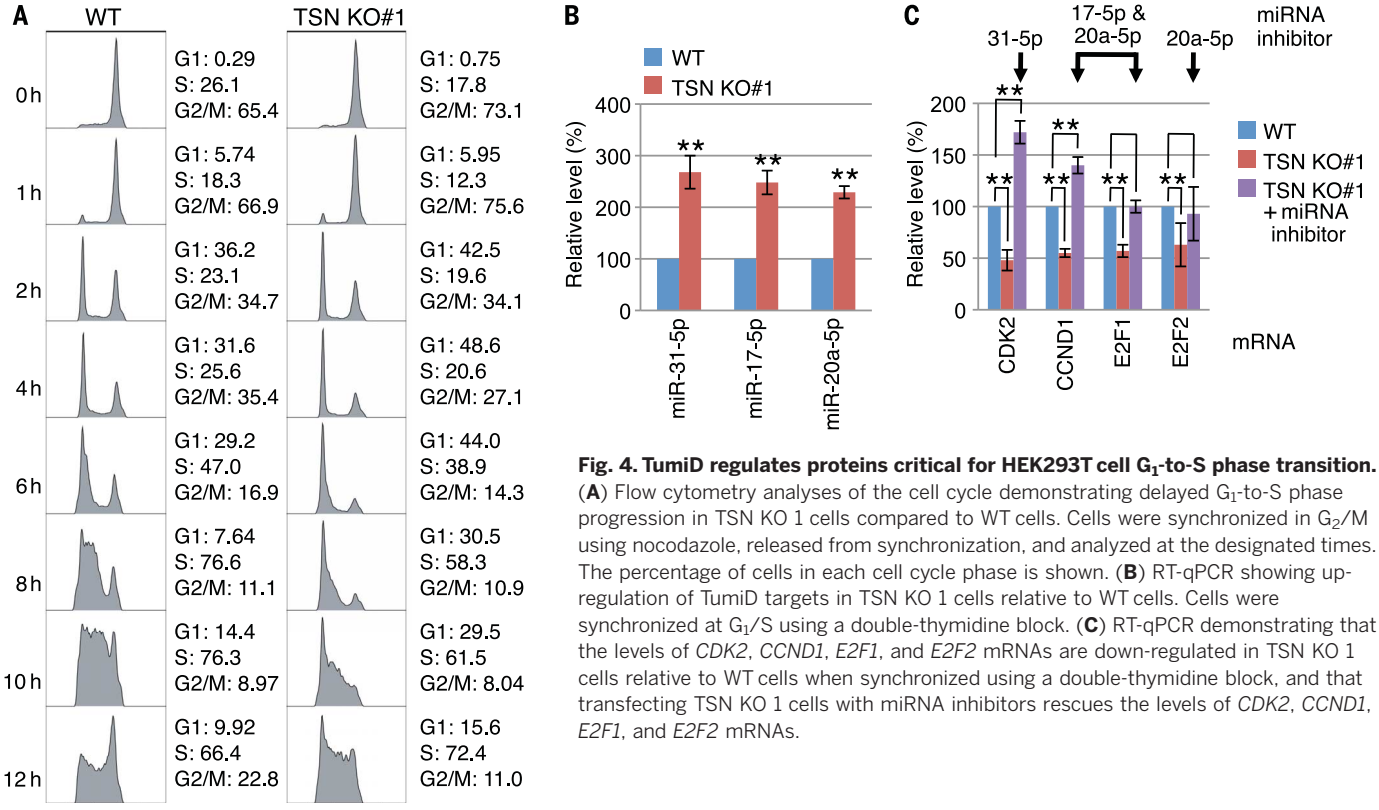

Fig. 4. TumiD regulates proteins critical for HEK293T cell G_1-to-S phase transition. (**A**) Flow cytometry analyses of the cell cycle demonstrating delayed G_1-to-S phase progression in TSN KO 1 cells compared to WT cells. Cells were synchronized in G_2/M using nocodazole, released from synchronization, and analyzed at the designated times. The percentage of cells in each cell cycle phase is shown. (**B**) RT-qPCR showing up-regulation of TumiD targets in TSN KO 1 cells relative to WT cells. Cells were synchronized at G_1/S using a double-thymidine block. (**C**) RT-qPCR demonstrating that the levels of *CDK2*, *CCND1*, *E2F1*, and *E2F2* mRNAs are down-regulated in TSN KO 1 cells relative to WT cells when synchronized using a double-thymidine block, and that transfecting TSN KO 1 cells with miRNA inhibitors rescues the levels of *CDK2*, *CCND1*, *E2F1*, and *E2F2* mRNAs.

regulatory proteins via TumiD. Although the level of *E2F3* mRNA was also down-regulated in TSN KO 1 cells, miRNA inhibitors did not restore the level of *E2F3* mRNA (fig. S22E), indicating that its down-regulation by TSN is not mediated by miR-17-5p or miR-20a-5p. Stably expressing FLAG-TSN in TSN KO cells rescued the expression levels of the three miRNAs and their target *CDK2*, *CCND1*, *E2F1*, and *E2F2* mRNAs (fig. S22, F and G).

Interestingly, E2F proteins promote transcription of the miR-17-92 cluster (*11*). Consistent with this, E2F1-3 knockdown in TSN KO 1 cells relative to wild-type cells was accompanied by a ~30% reduced level of pri-miR-17-92 but increased levels of miR-17-5p and miR-20a-5p in TSN KO cells because TumiD was inhibited (fig. S22H). Thus, TSN knockdown disrupts the tight control of mRNAs encoding cell cycle regulatory proteins via TumiD, offering an explanation for the elevated levels of TSN that can typify rapidly proliferating cells (*19*).

Our studies describe an endonuclease-mediated miRNA decay pathway that degrades specific miRNAs. In addition to adding an important dimension to how cellular miRNAs are regulated, these properties of TSN may be useful as a biochemical tool to degrade specific small RNAs in vitro.

REFERENCES AND NOTES

1. K. K. Reddi, *Nature* **187**, 74–75 (1960).
2. A. D. Scadden, *Nat. Struct. Mol. Biol.* **12**, 489–496 (2005).
3. W. Yang *et al.*, *Nat. Struct. Mol. Biol.* **13**, 13–21 (2006).
4. A. A. Caudy *et al.*, *Nature* **425**, 411–414 (2003).
5. S. M. Hammond, *FEBS Lett.* **579**, 5822–5829 (2005).
6. K. Augoff *et al.*, *Mol. Cancer Res.* **9**, 1500–1508 (2011).
7. J. Chou *et al.*, *Nat. Cell Biol.* **15**, 201–213 (2013).
8. M. Ha, V. N. Kim, *Nat. Rev. Mol. Cell Biol.* **15**, 509–524 (2014).
9. D. S. Schwarz, Y. Tomari, P. D. Zamore, *Curr. Biol.* **14**, 787–791 (2004).
10. B. K. Yoo *et al.*, *Hepatology* **53**, 1538–1548 (2011).
11. E. Mogilyansky, I. Rigoutsos, *Cell Death Differ.* **20**, 1603–1614 (2013).
12. O. S. Rissland, S. J. Hong, D. P. Bartel, *Mol. Cell* **43**, 993–1004 (2011).
13. C. Su *et al.*, *J. Biol. Chem.* **290**, 7208–7220 (2015).
14. F. A. Ran *et al.*, *Cell* **154**, 1380–1389 (2013).
15. H. S. Kim *et al.*, *Oncotarget* **6**, 8089–8102 (2015).
16. Z. Yu *et al.*, *J. Cell Biol.* **182**, 509–517 (2008).
17. K. A. O'Donnell, E. A. Wentzel, K. I. Zeller, C. V. Dang, J. T. Mendell, *Nature* **435**, 839–843 (2005).
18. Y. Sylvestre *et al.*, *J. Biol. Chem.* **282**, 2135–2143 (2007).
19. N. Jariwala *et al.*, *Int. J. Oncol.* **46**, 465–473 (2015).
20. D. Schmitter *et al.*, *Nucleic Acids Res.* **34**, 4801–4815 (2006).

ACKNOWLEDGMENTS

Raw data are deposited in the Gene Expression Omnibus (accession no. GSE77484). We thank F. Lopez for plasmid preparations; H. Siomi, K. Nishikura, and H. Yuan for plasmids; P. Svoboda for Dicer-kd 2b2 cells; M. Gleghorn for protein structure advice; A. Rosenberg for statistical analyses; and M. Popp for comments on the manuscript. Supported by NIH grants R37 GM74593 (L.E.M.), R01 GM084089 (B.T.), and P30 AR061307 (R.A.E.); the Uehara Memorial Foundation (K.M.); and the Mochida Memorial Foundation (K.M.). L.E.M. and R.A.E. are the inventors on U.S. provisional patent application 62/471627 filed 15 March 2017 by the University of Rochester (entitled "Compositions and Methods Targeting the TumiD Pathway for Treating and Preventing Cancer").

SUPPLEMENTARY MATERIALS

www.sciencemag.org/content/356/6340/859/suppl/DC1
Materials and Methods
Figs. S1 to S22
Tables S1 to S8
References (*21*–*35*)

2 September 2016; resubmitted 16 November 2016
Accepted 21 April 2017
10.1126/science.aai9372

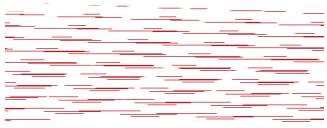

Tudor-SN–mediated endonucleolytic decay of human cell microRNAs promotes G $_1$/S phase transition

Reyad A. Elbarbary, Keita Miyoshi, Jason R. Myers, Peicheng Du, John M. Ashton, Bin Tian and Lynne E. Maquat (May 25, 2017)
Science **356** (6340), 859-862. [doi: 10.1126/science.aai9372]

Editor's Summary

Breaking down miRNAs

Although much work has examined microRNA (miRNA) biogenesis, relatively little is known about miRNA decay. Elbarbary *et al.* now identify Tudor-SN, an endonuclease that interacts with the RNA-induced silencing complex. Tudor-SN targets miRNAs at CA and UA dinucleotides located more than five nucleotides from miRNA ends. Tudor-SN-mediated miRNA decay removes miRNAs that silence genes encoding proteins that are critical for the G_1-to-S phase transition in the cell cycle.

Science, this issue p. 859

Science (print ISSN 0036-8075; online ISSN 1095-9203) is published weekly, except the last week in December, by the American Association for the Advancement of Science, 1200 New York Avenue NW, Washington, DC 20005.